

On Electron Transport in ZrB_{12} , ZrB_2 and MgB_2

V.A. Gasparov, M.P. Kulakov, N.S. Sidorov, and I.I. Zver'kova
*Institute of Solid State Physics RAS, 142432 Chernogolovka,
Moscow District, Russian Federation*

V.B. Filipov, A.B. Lyashenko, and Yu.B. Paderno
Institute for Problems of Material Science NANU, Kiev, Ukraine

(Dated: today)

We report on measurements of the temperature dependence of resistivity, $\rho(T)$, for single crystal samples of ZrB_{12} , ZrB_2 and polycrystalline samples of MgB_2 . It is shown that cluster compound ZrB_{12} behaves like a simple metal in the normal state, with a typical Bloch - Grüneisen $\rho(T)$ dependence. However, the resistive Debye temperature, $T_R = 300 \text{ K}$, is three times smaller than T_D obtained from specific heat data. We observe the T^2 term in $\rho(T)$ of these borides, which could be interpreted as an indication of strong electron-electron interaction. Although the $\rho(T)$ dependence of ZrB_{12} reveals a sharp superconductive transition at $T_c = 6.0 \text{ K}$, no superconductivity was observed for single crystal samples of ZrB_2 down to 1.3 K .

PACS numbers: 74.70.Ad, 74.60.Ec, 72.15.Gd

It is known that boron has a tendency to form cluster compounds. In particular there are octahedral B_6 clusters in MeB_6 , icosahedral B_{12} clusters in β -rhombohedral boron, and cubo-octahedral B_{12} clusters in MeB_{12} . So far, several superconducting cubic hexa - MeB_6 and dodecaborides - MeB_{12} have been discovered [1] ($\text{Me}=\text{Sc}, \text{Y}, \text{Zr}, \text{La}, \text{Lu}, \text{Th}$). Many other cluster borides ($\text{Me}=\text{Ce}, \text{Pr}, \text{Nd}, \text{Eu}, \text{Gd}, \text{Tb}, \text{Dy}, \text{Ho}, \text{Er}, \text{Tm}$) were found to be ferromagnetic or antiferromagnetic [1, 2]. Even though the superconductivity in ZrB_{12} was discovered a long time ago ($T_c = 6 \text{ K}$) [1], there has been little effort devoted to the study of electron transport and basic superconductive properties of dodecaborides. Only recently, the electron transport of solid solutions $\text{Zr}_{1-x}\text{Sc}_x\text{B}_{12}$ [3] as well as the band structure calculations of ZrB_{12} [4] has been reported. Understanding the properties of the cluster borides as well as the superconductivity mechanism in these compounds is very important.

Recently, we reported superconductivity at 5.5 K in the polycrystalline samples of ZrB_2 [5]. This was not confirmed in later studies [6]. It was recently suggested [7] that this observation could be associated with nonstoichiometry in the zirconium sub-lattice. In this letter we address this problem. We present the results from measurement of the temperature dependencies of resistivity, $\rho(T)$, for single crystals of ZrB_{12} and ZrB_2 . Comparative data from polycrystalline samples of MgB_2 are also presented. The superconducting properties of ZrB_{12} will be published elsewhere.

Under ambient conditions, dodecaboride ZrB_{12} crystallizes in the *fcc* structure of the UB_{12} type (space group *Fm $\bar{3}$ m*), $a = 0.7408 \text{ nm}$ [8]. In this structure, the Zr atoms are located at interstitial openings in the close-packed B_{12} clusters [3]. In contrast, ZrB_2 shows a phase consisting of two-dimensional graphite-like monolayers of boron atoms with a honeycomb lattice structure,

intercalated with Zr monolayers (with lattice parameters $a = 0.30815 \text{ nm}$ and $c = 0.35191 \text{ nm}$ [5]).

The ZrB_2 powder was produced by the boron carbide reduction of ZrO_2 . The ZrB_{12} single crystals were obtained from a mixture of a certain amount of ZrB_2 and an excess of boron (50 – 95%). The resulting materials were subjected to a crucible-free RF-heated zone-induction melting process in an argon atmosphere. The obtained single crystal ingots of ZrB_{12} and ZrB_2 have a typical diameter of about 5 – 6 mm and a length of 40 mm. A metallographic investigation detected that the ZrB_2 crystal is surrounded by a polycrystalline rim about 0.5 mm thick. The measured specific density of the ZrB_{12} rod is 3.60 g/cm^3 , in good agreement with the theoretical density. The X-ray diffraction measurements confirmed that both ingots are single crystal. We found the cell parameters of ZrB_{12} , $a = 0.74072 \pm 0.00005 \text{ nm}$, to be very close to the published values [8].

Polycrystalline MgB_2 and CaMgB_2 samples were sintered from metallic Mg or a mixture of Ca, Mg powders and boron pellets using a similar technique as outlined in our earlier work [5]. This technique is based on the reactive liquid Mg, Ca infiltration of boron. X-ray diffraction patterns and optical investigation show large grains of single MgB_2 phase, with much smaller grains of semiconducting CaB_6 phase visible in-between. Density of MgB_2 grains was rather high, 2.4 g/cm^3 , while the samples prepared from Mg infiltration had smaller density of 2.2 g/cm^3 . Only MgB_2 samples cut from large grains were studied. These samples will be denoted as CaMgB_2 .

We used a spark erosion method to cut the samples into a parallelepiped with dimensions of about $0.5 \times 0.5 \times 8 \text{ mm}^3$. Single crystal samples were oriented along $\langle 100 \rangle$ for ZrB_{12} , and in hexagonal $[0001]$ and basal $[1\bar{1}00]$ directions for ZrB_2 , respectively. The orientation process was performed using an X-ray Laue camera. The

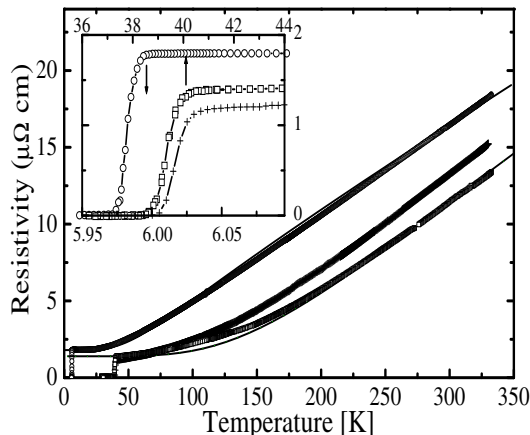


FIG. 1: Temperature dependence of the resistivity, $\rho(T)$, of ZrB_{12} single crystal (open circles), MgB_2 (squares) and CaMgB_2 (triangles) samples. The solid lines represent BG fits to the experimental data by Eq. 1.

samples were lapped by diamond paste and subsequently etched: ZrB_{12} in hot nitrogen acid, ZrB_2 in mixture of $\text{H}_2\text{O}_2/\text{HNO}_3/\text{HF}$, and MgB_2 in 2% HCl plus water-free ethanol.

A standard four-probe *ac* (9Hz) method was used for resistance measurements. We used *Epotek H20E* silver epoxy for electrical contacts. The samples were mounted in a temperature variable liquid helium cryostat. Temperature was measured with platinum (PT-103) and carbon glass (CGR-1-500) sensors. The critical temperature measured by RF susceptibility [5] and $\rho(T)$ was found to be $T_{c0} = 5.97 \text{ K}$ for ZrB_{12} samples and 39 K for MgB_2 polycrystalline samples, respectively.

We display the temperature dependence of the resistivity for ZrB_{12} , MgB_2 and CaMgB_2 in Fig. 1 and that of ZrB_2 in Fig. 2. To emphasize the variation of $\rho(T)$ in a superconductive state, we plot these data in the inset of Fig. 1. The samples demonstrate a remarkably narrow superconducting transition with $\Delta T = 0.04 \text{ K}$ for ZrB_{12} and with $\Delta T = 0.7 \text{ K}$ for both MgB_2 samples. Such a transition is a characteristic of good quality samples.

As we can see from Fig. 2, no superconductivity was observed in ZrB_2 down to 1.3 K , while a pronounced slope change in $\rho(T)$ is observed around 7 K . One can explain such behavior in the following way. In ZrB_2 the Fermi level is located in the pseudo gap. The presence of Zr defects in $\text{Zr}_{0.75}\text{B}_2$ leads to the appearance of a very intense peak in the density of states in the vicinity of the pseudo gap and subsequent superconductivity [7]. We strongly believe that the observation of [5] was due to nonstoichiometry of our samples. Superconductivity in nonstoichiometric samples is very common in other borides: $\text{MoB}_{2.5}$, $\text{NbB}_{2.5}$, Mo_2B , W_2B , $\text{BeB}_{2.75}$ [9, 10].

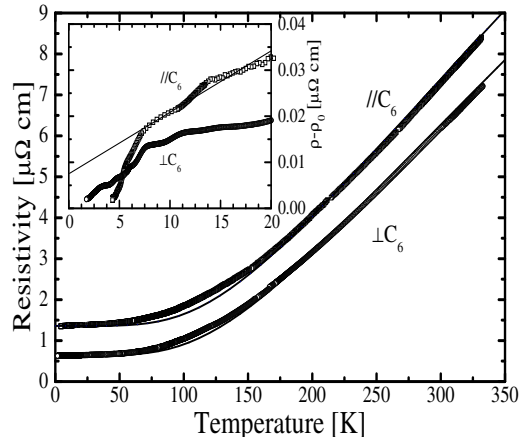


FIG. 2: Temperature dependence of $\rho(T)$ of ZrB_2 single crystal samples in basal plane (circles) and in *c* direction (squares).

It is worth noting that ZrB_{12} is mostly boron, and one could speculate that its resistivity should be rather high. In contrast we observe that the room temperature resistivity of ZrB_{12} is almost the same as for MgB_2 and ZrB_2 samples. The $\rho(T)$ is linear above 90 K with the slope of $\rho(T)$ more pronounced than in MgB_2 or ZrB_2 . The residual resistivity ratio RRR of 9.3 for ZrB_{12} as well as $\text{RRR} \approx 10$ for MgB_2 and ZrB_2 samples suggests that the samples are in the clean limit. One can predict a nearly isotropic resistivity for *fcc* ZrB_{12} , which can be described by the Bloch-Grüneisen (BG) expression of the electron-phonon *e-p* scattering rate [11]:

$$\rho(t) - \rho(0) = 4\rho_1 t^5 \int_0^{1/t} \frac{x^5 e^x dx}{(e^x - 1)^2} = 4\rho_1 t^5 J_5(1/t) \quad (1)$$

Here, $\rho(0)$ is the residual resistivity, $\rho_1 = d\rho(T)/dT$ is a slope of $\rho(T)$ at high T ($T > T_R$), $t = T/T_R$, T_R is the resistive Debye temperature and $J_5(1/t)$ is the Debye integral. As we can see from Fig. 1, all data for ZrB_{12} fall very close to the theoretical BG function (solid line). To emphasize the variation of $\rho(T)$ at low T we plot these data as $\rho(T) - \rho(0)$ versus $t^5 J_5(1/t)$ in Fig. 3 on a log-log scale. The BG formula predicts a linear dependence of $\log[\rho(T) - \rho(0)]$ versus $\log[t^5 J_5(1/t)]$ with the slope equal to unity. We use T_R as a fitting parameter to achieve agreement at the high temperatures. For comparison, we also present our $\rho(T)$ data of ZrB_2 and MgB_2 calculated in a clean case of the two band model [12].

It is clear from Fig. 3 that above 25 K the BG model describes the $\rho(T)$ dependence of ZrB_{12} fairly well. It is remarkable that this description works well with constant $T_R = 300 \text{ K}$. At the same time, T_D calculated from specific heat data [13] is three times higher. Furthermore

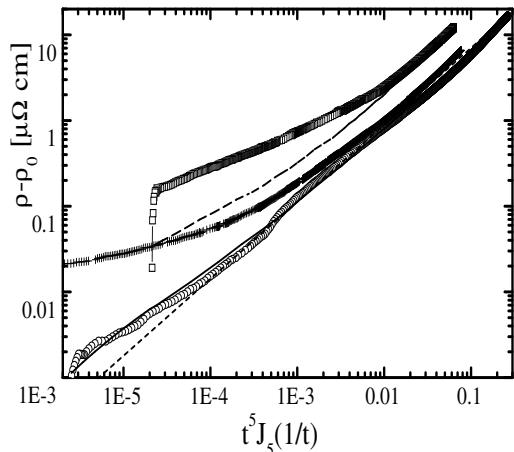


FIG. 3: The $\rho(T) - \rho(0)$ vs. reduced Debye integral $t^5 J_5(1/t)$ for ZrB_{12} (open circles), ZrB_2 in basal plane (crosses) and CaMgB_2 (squares). The dashed line is $\rho(T)$ of MgB_2 calculated in the two band model [12].

T_D increases from 800 K to 1200 K as temperature varies from T_c up to room temperature. In order to shed light on this discrepancy, we used a model applied to LaB_6 of Ref. [14]. We can treat the boron sub-lattice as a Debye solid with T_R and the Zr ions as independent Einstein oscillators with characteristic temperature T_E . The effect of the Einstein mode on the resistivity of a metallic solid is discussed in Ref.[15]:

$$\rho_E(T) = \frac{KN \cdot e^{T_E/T}}{M \cdot T(e^{T_E/T} - 1)^2}. \quad (2)$$

Here N is the number of oscillators per unit volume, K is a constant that depends on the electron density of the metal, M is the atomic mass. We fit the data by summing Eq. (1) and Eq. (2), and living KN/M , ρ_1 , T_R as free parameters. Although the model calculations perfectly match the data (see solid line in Fig. 3), the T_E we are getting is unreasonably small ($T_E = 50$ K), and the difference between T_R and specific heat T_D becomes even worse, $T_R = 270$ K. We believe that this inconsistency of T_R and T_D can be explained by limitation of T_R by a cut-off phonon wave vector $q = k_B T / \hbar s$. The latter is limited by the Fermi surface (FS) diameter $2k_F$ [16] rather than the highest phonon frequency in the phonon spectrum.

According to band structure calculations [4], the FS of ZrB_{12} consists of an open sheet along ΓL direction at point Γ with $k_{\Gamma X} = 0.47 \text{ \AA}^{-1}$, a quasi spherical sheet at point X ($k_{X\Gamma} = 0.37 \text{ \AA}^{-1}$) and a small sheet at point K ($k_{K\Gamma} = 0.14 \text{ \AA}^{-1}$). We suggest that T_R is limited by the small FS sheet. Unfortunately the experimental FS model and the sound velocity are not yet known.

Therefore we can not corroborate this suggestion by experimental FS.

As we can see from Fig. 3, the $\rho(T)$ of ZrB_2 and MgB_2 samples deviates from the BG model even more dramatically. Putti *et al.* [17] modified the BG equation introducing variable power n for the $t^n J_n(1/t)$ term in Eq. (1). The best fit to the data was obtained with $n = 3$ which in fact ignores a small angle e - p scattering. Recently Sologubenko *et al.* [18] reported a cubic T dependence in the a, b plane resistivity below 130 K in the single crystals of MgB_2 . This was attributed to the interband e - p scattering in transition metals.

However, we believe there are strong objections to this modified BG model: (i) a cubic $\rho(T)$ dependence is a theoretical model for large angle e - p scattering and no evidence of it was observed in transition and non-transition metals; (ii) the numerous studies of the $\rho(T)$ dependence in transition metals have been found to be consistent with a sum of electron-electron e - e , T^2 , and e - p , T^5 , contributions to the low T resistivity, which may easily be confused with a T^3 law [11, 19, 20]; (iii) the interband $\sigma - \pi$ e - p scattering plays no role in normal transport in the two band model for MgB_2 [12].

In order to solve these problems, we added e - e scattering T^2 term in Eq. (1) [19, 20] as a possible scenario. Indeed, keeping in mind that the BG term is proportional to T^5 at $T < 0.1T_R$, $\rho(T)$ dependence may be presented in a simple way [19, 20]: $[\rho(T) - \rho(0)]/T^2 = \alpha + \beta T^3$. Here α and $\beta = 497.6\rho_1/T_R^5$ are parameters of e - e and e - p scattering terms, respectively. Such a plot should yield a straight line with slope of β and its intercept with y-axis ($T = 0$) should equal to α . Further, to be consistent with BG law, the β parameter should lead to the same T_D as obtained from high T log-log fit in Fig. 3, and both coefficients must be independent of $\rho(0)$. We determined $\rho(0)$ from the intercept of linear $\rho(T)$ vs T^2 dependence with the $T = 0$ axis and plotted the $[\rho(T) - \rho(0)]/T^2$ vs. T^3 in Fig. 4. It is evident that the measured resistivity approaches a quadratic law at $T < 25$ K in ZrB_{12} , at $T < 100$ K in ZrB_2 , and at $T < 150$ K in both MgB_2 samples.

The regime of applicability of two term fit is limited to temperatures below $0.1T_R$. At larger T the e - p term increases more slowly than T^5 law and this is why the data are not consistent any more with the two terms equation. From the intercept with $T = 0$ axis, we find very similar values of α for ZrB_{12} and ZrB_2 samples in the basal plane ($\alpha = 22 \text{ p}\Omega\text{cmK}^{-2}$ and $15 \text{ p}\Omega\text{cmK}^{-2}$, respectively) while α is about five times larger for CaMgB_2 sample, $95 \text{ p}\Omega\text{cmK}^{-2}$. The slopes of β give ρ_1 and T_R values largely consistent with high temperature log-log fits for the ZrB_{12} and ZrB_2 samples.

However, low T results for β and ρ_1 are far from consistent with high T data for both MgB_2 and CaMgB_2 samples. Nevertheless, the magnitude of $T_R = 900$ K for MgB_2 extracted from log-log fit above 150 K, is in excellent agreement with $T_D = 920$ K obtained from low-temperature specific heat measurements [21], and is

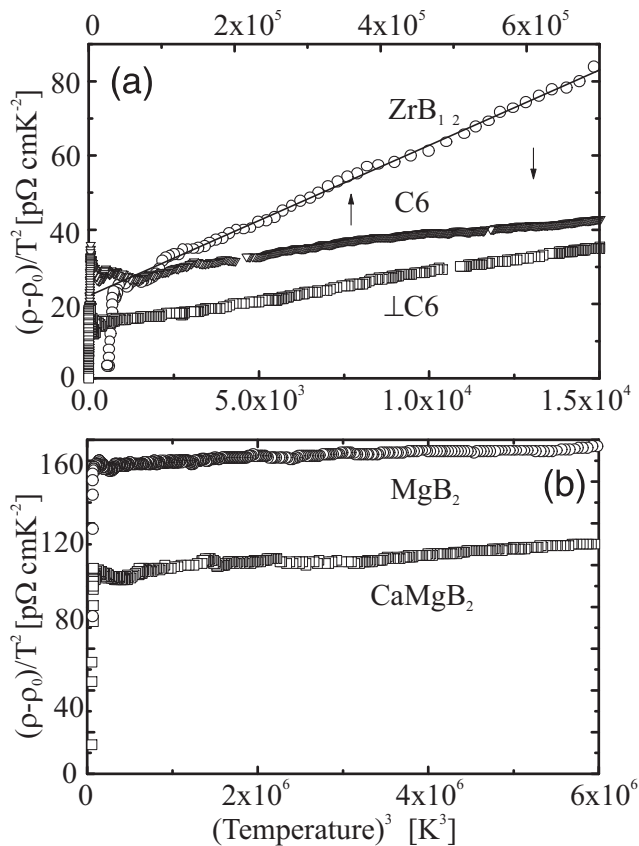


FIG. 4: Low temperature behavior of $[\rho(T) - \rho(0)]/T^2$ versus T^3 for: (a) ZrB_{12} (circles), ZrB_2 in basal plane (squares), ZrB_2 along c (triangles) and (b) MgB_2 (circles) and CaMgB_2 (squares) samples.

considerably lower than the reported data based on T^3 dependence of $\rho(T)$ ($T_R = 1050 - 1226 \text{ K}$, where T^2 term was ignored. [6, 17, 18]). A similar fit for theoretical curve is even more consistent with $T_R = 900 \text{ K}$, however we have to mention that violation of Matthiessen's rule in MgB_2 may mask the intrinsic $\rho(T)$ dependence [12].

In general, there are many scattering processes responsible for the T^2 term in $\rho(T)$ of metals: (i) size, surface, dislocation and impurity scattering induced deviations from Matthiessen's rule (see references in [22]); (ii) e - p scattering for small cylindrical FS sheets relative to the phonon wave vector [16]; (iii) inelastic electron impurity scattering (e - i) [23]; (iv) the quantum interference between e - i and e - p scattering [24]; (v) e - e scattering [19, 20].

We can estimate some of these effects. We use Drude law to obtain the residual electron mean free path $l = 4\pi v_F / \rho \omega_p^2$. Using a Fermi velocity of $v_F = 3.2 \cdot 10^7 \text{ cm/s}$ and a plasma frequency $\omega_p^\sigma = 5.16 \cdot 10^{15} \text{ s}^{-1}$ for MgB_2 σ -band [12], we obtain $l \approx 100 \text{ nm}$. This implies that size effects are negligible for both MgB_2 samples and Zr

borides. In agreement with ZrB_2 data (see Fig. 4) the α is proportional to $\rho(0)$ for inelastic e - i scattering [23, 24]. However, this term is 1.5 times lower for CaMgB_2 relative to MgB_2 , which has the same $\rho(0)$.

We can try to estimate contribution from the small FS sheets to α . The T^2 term was observed in $\rho(T)$ and electron scattering rates of Bi and Sb, which was attributed to a missing of one q component for e - p scattering on small cylindrical FS sheets [16]. The FS of MgB_2 is composed of two warped open cylinders running along the c axis, which arise from σ boron orbitals [12, 25]. The FS of ZrB_2 consist of nearly ellipsoidal surfaces joined together at the corners [26, 27], which may also be responsible for the T^2 term in $\rho(T)$. We can use the sound velocity $s = 1.1 \cdot 10^6 \text{ cm/s}$ and $8 \cdot 10^5 \text{ cm/s}$ for MgB_2 and ZrB_2 , respectively [28, 29], to estimate the lowest temperature, $T_{min} = \hbar k_F s / k_B$, when the phonon wave vector q matches a neck of smaller σ tube in MgB_2 ($k_\sigma = 0.129 \text{ \AA}^{-1}$ [25]) or a diameter of the ellipsoidal sheets in ZrB_2 ($k_F = 0.095 \text{ \AA}^{-1}$ [26]). We obtain $T_{min} = 95 \text{ K}$ and 60 K , respectively. Thus we conclude that $q < k_F$ at $T < 100 \text{ K}$ in both diborides, which implies that the contribution of the 2D FS sheets to α is negligible.

In general only umklapp e - e scattering contributes to $\rho(T)$, whereas the normal collisions are significant in compensated metals and in thermal resistivity [20]. Borides have rather high T_D which depresses the e - p scattering, so that the e - e SR term is easier to observe. Notice however that the α value for MgB_2 is five times larger than corresponding values in ZrB_{12} and ZrB_2 . The latter values are in turn five times larger than in transition metals ($\alpha_{Mo} = 2.5 \text{ p}\Omega \text{ cm}/\text{K}^2$ and $\alpha_W = 1.5 - 4 \text{ p}\Omega \text{ cm}/\text{K}^2$ [19, 20]). Therefore, additional experiments must be performed for more pure samples before final conclusion about the origin of the T^2 term in borides can be drawn.

In conclusion, we present a study of the $\rho(T)$ of single crystals of ZrB_{12} , ZrB_2 and polycrystalline samples of MgB_2 . Large differences between resistive and specific heat Debye temperatures have been observed for ZrB_{12} . The results provide evidence of a T^2 term for all these borides at low T , whose origin is not yet understood.

Acknowledgments

Very useful discussions with V.F. Gantmakher, A. Junod, I. Shein, R. Huguenin, and help in paper preparation of L.V. Gasparov are gratefully acknowledged. This work was supported by the Russian Scientific Programs: Superconductivity of Mesoscopic and Highly Correlated Systems (Volna 4G); Synthesis of Fullerenes and Other Atomic Clusters (No.541-028); Surface Atomic Structures (No.4.10.99), Russian Ministry of Industry, Science and Technology (MSh-2169.2003.2), RFBR (No.02-02-16874-a) and by the INTAS (No.01-0617).

-
- [1] B.T. Matthias, T.H. Geballe, K. Andres, E. *et al.*, Science **159**, 530 (1968).
- [2] Yu.B. Paderno, N. Shitsevalova, I. Batko, *et al.*, J. Alloys Comp. **219**, 215 (1995).
- [3] K. Hamada, M. Wakata, N. Sugii *et al.*, Phys. Rev. B **48**, 6892 (1993).
- [4] I.R. Shein and A.L. Ivanovskii, Physics of the Solid State **45**, 1429 (2003); [Fizika Tverdogo Tela **45**, 1363 (2003)].
- [5] V.A. Gasparov, N.S. Sidorov, I.I. Zver'kova *et al.*, JETP Letters **73**, 601 (2001).
- [6] B. Fisher, K.B. Chashka, L. Patlagan, *et al.*, Physica C **384**, (2003) 1.
- [7] I.R. Shein, N.I. Medvedeva, and A.L. Ivanovskii, Physics of the Solid State **45**, 1617 (2003), [Fizika Tverdogo Tela **45**, 1541 (2003)].
- [8] A. Leithe-Jasper, A. Sato, T. Tanaka, *et al.*, NCS **217**, 319 (2002).
- [9] Z. Fisk, AIP Conf. Proc. **#231** (1991).
- [10] A. Yamamoto, C. Takao, T. Masui *et al.*, Physica C **383**, 197 (2002).
- [11] J.M. Ziman, Electrons and Phonons, Theory of Transport Phenomena in Solids (Oxford U.P., Oxford, England, 1960).
- [12] I.I. Mazin, O.K. Andersen, O. Jepsen, *et al.*, Phys. Rev. Lett. **89**, 107002 (2002).
- [13] A. Junod, *et al.*, (to be published, 2004).
- [14] D. Mandrus, B.C. Sales, and R. Jin, Phys. Rev. B **64**, 012302 (2001).
- [15] J.R. Cooper, Phys. Rev. B **9**, 2778 (1974).
- [16] V.F. Gantmakher, Rep. Progr. Phys. **37**, 317 (1974).
- [17] M. Putti, E. Galleani, D. Marr'e, *et al.*, Eur. Phys. J. B **25**, 439 (2002).
- [18] A.V. Sologubenko, J. Jun, S.M. Kazakov *et al.*, Phys. Rev. B **66**, 014504 (2002).
- [19] N.V. Vol'kenshtein, V.P. Dyakina, V.E. Startsev, phys. stat. sol. **57**, 9 (1973).
- [20] V.A. Gasparov and R. Huguenin, Adv. Phys. **42**, 393 (1993).
- [21] A. Junod, Y. Wang, F. Bouquet *et al.*, in: Studies of High Temperature Superconductors, Vol.38, Editor A. Narlikar, Nova Science Publishers, Commack (N.Y.) 2002, p.179.
- [22] J. van der Maas and R. Huguenin, J. Phys.: Condens. Matter **2**, 8137 (1990).
- [23] Yu. Kagan and A.P. Zhernov, Zh. Eksp. Teor. Fiz. **50**, 1107 (1966), [Sov. Phys. JETP **23**, 737 (1966)].
- [24] M.Yu. Reizer and A.V. Sergeev, Zh. Eksp. Teor. Fiz. **92**, 2291 (1987), [Sov. Phys. JETP **65**, 1291 (1987)].
- [25] A. Carrington, P.J. Meeson, J.R. Cooper, *et al.*, Phys. Rev. Lett. **91**, 037003 (2003).
- [26] T. Tanaka, Y. Ishizawa, E. Bannai *et al.*, Sol. St. Commun. **26**, 879 (1978).
- [27] H. Rosner, J. M. An, W. E. Pickett, *et al.*, Phys. Rev. B **66**, 24521 (2002).
- [28] A. Shukla, M. Calandra, M. d'Astuto, *et al.*, Phys. Rev. Lett. **90**, 095506 (2003).
- [29] T. Aizawa, W. Hayami, and S. Otani, Phys. Rev. B **65**, 024303 (2001).